

MVGrasp: Real-Time Multi-View 3D Object Grasping in Highly Cluttered Environments

Hamidreza Kasaei¹, Mohammadreza Kasaei²

Abstract—Nowadays service robots are entering more and more in our daily life. In such a dynamic environment, a robot frequently faces pile, packed, or isolated objects. Therefore, it is necessary for the robot to know how to grasp and manipulate various objects in different situations to help humans in everyday tasks. Most state-of-the-art grasping approaches addressed four degrees-of-freedom (DoF) object grasping, where the robot is forced to grasp objects from above based on grasp synthesis of a given top-down scene. Although such approaches showed a very good performance in predefined industrial settings, they are not suitable for human-centric environments as the robot will not be able to grasp a range of household objects robustly, for example, grasping a bottle from above is not stable. In this work, we propose a multi-view deep learning approach to handle robust object grasping in human-centric domains. In particular, our approach takes a partial point cloud of a scene as an input, and then, generates multi-views of existing objects. The obtained views of each object are used to estimate pixel-wise grasp synthesis for each object. To evaluate the performance of the proposed approach, we performed extensive experiments in both simulation and real-world environments within the pile, packed, and isolated objects scenarios. Experimental results showed that our approach can estimate appropriate grasp configurations in only 22ms without the need for explicit collision checking. Therefore, the proposed approach can be used in real-time robotic applications that need closed-loop grasp planning.

I. INTRODUCTION

Industrial robots have mainly designed to perform repetitive tasks in controlled environments. Recent years have seen increasing interest in deploying service robots to human-centric environments. In such unstructured settings, object grasping is a challenging task due to the high demand for real-time and accurate responses for a vast number of objects with a wide variety of shapes and sizes under various clutter and occlusion conditions. Although several grasping approaches have been developed successfully for 4DoF (x, y, z, θ) , many challenges still remain towards dexterous robust grasping. One major obstacle to achieving real-time object grasping is the cost of collecting efficient training data by real robots through self-supervised trial and error experiments. To address this challenge, recent works in grasp synthesis have mainly focused on developing end-to-end deep convolutional learning-based approaches to plan grasp configuration directly from sensor

data. Although it has been proven that these approaches can outperform hand-crafted grasping methods, the grasp planning is mainly constrained to top-down grasps from a single depth sensor [1], [2]. These approaches assume a favorable global camera placement and force the robot to grasp objects from a single direction, which is perpendicular to the image plane. Such constraints bound the flexibility of the robot, and the robot will not be able to grasp a range of household objects robustly, e.g., bottles, boxes, etc. Furthermore, a certain set of objects has convenient parts to be grasped, e.g., the ear of a mug, or in some situation, it is easier to approach a household object from different directions.

In this work, we propose a multi-view deep learning approach to handle real-time object grasping. Figure 1 depicts an overview of our work. In particular, our approach takes a partial point cloud of a scene as an input. We then generate multi-view depth images of the objects and import them into a view selection function. The best view is then fed to a deep network to estimate a pixel-wise grasp synthesis (grasp quality, orientation, and width of a grasp). It is worth mentioning that we trained the network end-to-end using a very small isolated object grasping dataset. We based our approach on the hypothesis that considering multi-view of the objects forces the network to capture collisions among the gripper, objects, and the environment, which is necessary for object manipulation in human-centric environments. We validate this hypothesis by performing several experiments in both simulated and real-robot settings. More specifically, we evaluate the performance of the proposed method on the isolated, pile, and packed objects scenarios. Extensive quantitative and qualitative evaluations showed that our approach significantly improved the state-of-the-art methods. Our approach, on average, could estimate stable grasp configurations in less than 22ms without the need for explicit collision checking. Therefore, the proposed approach is suitable to be used in real-time robotic applications that need closed-loop grasp planning.

II. RELATED WORK

Traditional object grasping approaches explicitly model how to grasp different objects mainly by considering prior knowledge about object shape, and pose [3]. It has been proven that it is hard to obtain such prior information for never-seen-before objects in human-centric environments [4]. More recent approaches try to tackle this limitation by formulating object grasping as an *object-agnostic* problem, in which grasp synthesis is detected based on learned visual features without considering prior *object-specific* information. Therefore, these

¹Department of Artificial Intelligence, Bernoulli Institute, University of Groningen, 9747 AG, The Netherlands. Email: hamidreza.kasaei@rug.nl

²IEETA/DETI, University of Aveiro 3810-193 Aveiro, Portugal. Part of the work has been done, while the author was on an internship at the Department of AI, University of Groningen. Email: mohammadreza@up.pt

We thank NVIDIA Corporation for their generous donation of GPUs which was partially used in this research.

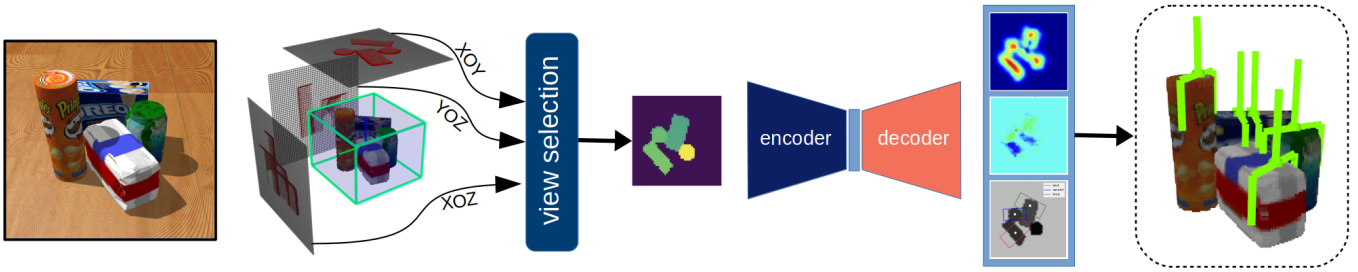


Fig. 1. Overview of the proposed approach: we designed a mixed autoencoder for multi-view object grasping to be used in both isolated and highly crowded scenarios. First, multiple views of a given object are generated. The view selection module selects which view is the best one in terms of grasping and then fed it to the grasp network to obtain a pixel-wise grasp synthesis. As shown in the most right part of the figure, the best grasp configurations are finally ranked and transformed from 2D to 3D using a set of known transformations.

approaches are able to generalize the learned grasping policies to new objects without the need for having the full model of the object in advance. In this vein, much attention has been given to object grasping approaches based on Convolutional Neural Network (CNN) [1], [5]–[7].

Deep-learning approaches for object grasping falling into three main categories depending on the input to the network. First, there are volume-based approaches [7], [8], where the object is represented as a 3D voxel grid and then fed to a CNN with 3D filter banks. Second, there are pointset-based approaches [9], [10], which directly use point cloud data as input. The final category is view-based approaches that receive the point cloud of the object and generate multiple views of the object. Our work belongs to this category. These approaches appear to be most effective in 3D object recognition and grasping, as shown by [1], [6], [11]–[16]. In these approaches, 2D images are extracted from the 3D representation by projecting the object’s points onto 2D planes, and then fed to a CNN to generate grasp syntheses. Finally, the robot executes the highest-ranked grasp [1]. One of the biggest bottlenecks with recent deep learning-based object grasping approaches is the execution time and sensitivity to calibration errors. Most of the approaches take a very long time to sample and rank grasp candidates individually [1], [5]. Unlike our approach, these approaches mainly designed to be used in open-loop control scenarios and are not suitable for real-time robotic applications.

There are some approaches that addressed closed-loop object grasping. These methods continuously receive visual inputs and update grasp configuration during execution mainly based on visual serving. Most of these methods considered several constraints to reduce the amount of required training data. For example, Morrison et al., [6] proposed Generative Grasping CNN (GG-CNN), a solution where grasp poses are generated for every pixel using a small CNN. Similar to our approach, GG-CNN is designed to be used for real-time closed-loop control using eye-in-hand visual feedback. Unlike GG-CNN, our approach works in an eye-to-hand system, resulting in a global view that is better suited for real-world applications where the robot has to consider an entire scene and not just a narrow top-down view. DexNet [1] and QT-Opt [4] learn only top-down grasping based on images from a fixed static camera. GG-CNN [6], DexNet [1], and QT-Opt [4], generate a grasp map per scene. Unlike these approaches, our approach generates a grasp synthesis map per object. Fur-

thermore, these approaches only work for top-down camera-settings and have mainly focused on solving 4DoF (x, y, z, yaw) grasping, where the gripper is forced to approach objects from above. The major drawbacks of these approaches are inevitably restricted ways to interact with objects. Moreover, the robot is not able to immediately generalize to different task configurations without extensive retraining. We tackle these problems by proposing a multi-view approach for object grasping in highly crowded scenarios.

Recent researches on multi-view grasping [17], [18], have been done using a single camera moving over a predefined trajectory, where each point of the trajectory is considered as a view. In [17], the most informative view is then chosen by means of entropy measures. In our work, we instead generate multiple views of the object and use the most informative view based on a viewpoint entropy measure for grasping.

III. PROBLEM FORMULATION

In this work, we formulate grasp synthesis as a learning problem of planning parallel-jaw grasps for objects in clutter. In particular, we intend to learn a function that receives a collection of rendered depth images of a 3D object as input, and returns (i) the best approaching direction, and (ii) a grasp map representing per-pixel grasp configuration for a selected view. The grasp map is then used to find the best grasp configuration for removing a target object from the workspace. In this work, we assume that the object has been segmented from a scene, and refer the reader to our previous works for this purpose [19].

A. Generating multiple views of objects

A three-dimensional (3D) object is usually represented as point cloud, $p_i : i \in \{1, \dots, n\}$, where each point is described by their 3D coordinates $[x, y, z]$. To capture depth images from a 3D object, we need to set up a set of virtual cameras around the object, where the \mathbf{Z} axes of cameras are pointing towards the centroid of the object. We first calculate the geometric center of the object as the average of all points of the object. Then, a local reference frame is created by applying principal component analysis on the normalized covariance matrix, Σ , of the object, i.e., $\Sigma \mathbf{V} = \mathbf{E} \mathbf{V}$, where $\mathbf{E} = [e_1, e_2, e_3]$ contains the descending sorted eigenvalues, and $\mathbf{V} = [\vec{v}_1, \vec{v}_2, \vec{v}_3]$ shows the eigenvectors. Therefore, \vec{v}_1 , shows the largest variance of the points of the object. In this work, \vec{v}_1 and the negative of the

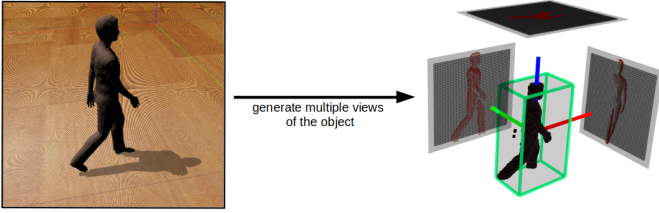


Fig. 2. An illustrative example of generating multiple views for an object: (left) a human-toy objects in Gazebo environment; (right) Point cloud of the object, its bounding box, local reference frame, and three projected views.

gravity vector are considered as \mathbf{X} and \mathbf{Z} axes, respectively. We define the \mathbf{Y} axis as the cross product of $\vec{v}_1 \times \mathbf{Z}$. The object is then transformed to be placed in the reference frame.

From each camera pose, we map the point cloud of the object into a depth image based on the truncated signed distance function (TSDF), an N^2 image grid, M , where each pixel p_i represents the truncated signed distance to the nearest surface. In particular, we first project the object to a square plane, M , centered on the camera's center. The projection area is then divided into $l \times l$ square grid, where each bin is considered as a pixel. Finally, the minimum z of all points falling into a bin is used as the pixel value. The size of the projection square area, $l \times l$, is an important factor for object grasping tasks. In the case of object-agnostic grasping, since the grasp configurations depend on the pose and size of the target object, a view of the object should not be scale-invariant, we consider a fixed size projection plane ($l \times l$). In our setup, the size of each side of the plane is defined as $l = k \times f_g$, where k is the number of pixels, and f_g represents the size of the head of the robot's finger, which is used to define the size of each pixel in the meter scale.

The number of object views is an important parameter for object grasping. In this work, we consider orthographic views including XoY, XoZ, and YoZ projections. An illustrative example of this procedure for a human-toy object is provided in Fig. 2. The intuition behind this selection is that most of the household objects are stably graspable from *top*, *side*, or *front* views [20]. The obtained projections are then normalized (i.e., mean-subtracted and divided by standard deviation) and fed to the network.

We develop a function to define which of these views is the best-view for approaching and grasping the target object. We consider the kinematic feasibility and distance that the robot would require to travel in the configuration space. In the case of large objects, or a pile of objects, there is a clear advantage (e.g., collision-free) to grasp from above, while for a single normal object (cans, bottles, boxes, toys), it completely depends on the pose of the object relative to the camera (see Fig. 3). Therefore, we use viewpoint entropy that nicely takes into account both the number of occupied pixels and their values. We calculate the entropy of a view, v , as $H(M) = -\sum_{i=1}^{l^2} p_i \log_2(p_i)$, where p_i represents the value

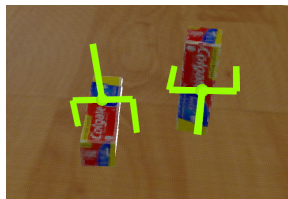


Fig. 3. Example of grasping a Colgate box in two different situations.

of i th pixel. The gripper finally approaches the object in an orthogonal direction to the view. It should be noted that the view selection function can be easily adapted to any other tasks and scenarios related criteria.

B. Network architecture

We aim to learn a function that maps an input object's view to multiple outputs representing pixel-wise antipodal grasp configurations, $f_\theta : \mathcal{X} \rightarrow \mathcal{Y}$. Towards this goal, we have designed a convolutional autoencoder that receives a depth image with height h and width w as input, $x_i \in \mathbb{R}^{h \times w}$, and returns a pixel-wise grasp configuration map, \mathbf{G}_i , i.e., $y_i = [\mathbf{G}_i]$. Since we want to use the network in a closed-loop control scenario, we add a constraint on number of trainable parameters to be less than 150K.

The network is parameterized by its weights θ . Our model is a single-input multiple-outputs network and is constructed using three types of layers, including convolution, deconvolution, and batch normalization.

The encoder part is composed of six convolutional layers (C1 to C6). We use a Rectified Linear Unit (ReLU) as the activation function of all layers of the encoder part to force the negative values to zero and eliminating the vanishing gradient problem which is observed in other types of activation functions. We added a batch normalization layer after each convolutional layer to stabilize the learning process and reducing the number of training epochs by keeping the mean output and standard deviation close to 0 and 1, respectively. The decoder part is composed of six transposed convolutional layers (T1 to T6), followed by three separate output layers for predicting grasp quality, width, and rotation. Similar to the encoder part, we use the ReLU activation function for all layers and add a batch normalization after each layer. We use the same padding in all convolution and transposed convolution layers to make the input and output be of the same size (see Section IV).

In this work, an antipodal grasp point is represented as a tuple, $g_i = \langle (u, v), \phi_i, w_i, q_i \rangle$, where (u, v) stands the center of grasp in image frame, ϕ_i represents the rotation of the gripper around the Z axis in the range of $[-\frac{\pi}{2}, \frac{\pi}{2}]$, w_i shows the width of the gripper where $w_i \in [0, w_{max}]$, and the success probability of the grasp is represented by $q_i \in [0, 1]$. Given an input view, the network generates multiple outputs, including: $(\phi, \mathbf{W}, \mathbf{Q}) \in \mathbb{R}^{h \times w}$, where pixel value of images indicate the measure of ϕ_i, w_i, q_i respectively. Therefore, from $f_\theta(I_i) = \mathbf{G}_i$, the best grasp configuration, g^* , is the one with maximum quality, and its coordinate indicate the center of grasp, i.e., $(u, v) \leftarrow g^* = \text{argmax}_{\mathbf{Q}} \mathbf{G}_i$. Given a grasp object dataset, \mathcal{D} , containing n_d images, $\mathcal{D} = \{(x_i, y_i) | 1 \leq i \leq n_d\}$, our model can be trained end-to-end to learn $f_\theta(\cdot)$.

After obtaining the grasp map of an input view, the Cartesian position of the selected grasp point, (u, v) , can be transformed to object's reference frame since the transformation of the orthographic view relative to the object is known. The depth value of the grasp point is estimated based on the minimum depth value of the surrounding neighbors of (u, v) that are within a radius of Δ , where $\Delta = 5\text{cm}$.

IV. EXPERIMENTAL RESULTS

We performed several rounds of simulation and real-robot experiments to evaluate the performance of the proposed approach. We were pursuing three goals in these experiments: (i) evaluating the performance of object grasping in three scenarios; (ii) investigating the usefulness of formulating object grasping as an object-agnostic problem for general purpose tasks; (iii) determine whether the same network can be used in both simulation and real-robot systems without additional fine-tuning. Towards this goal, we employed the same code and network (trained on the Cornell dataset) in both real and simulation experiments. All tests were performed with a PC running Ubuntu 18.04 with a 3.20 GHz Intel Xeon(R) i7, and a Quadro P5000 NVIDIA.

A. Network design analysis

We trained several networks with the proposed architecture but different parameters including filter size, dropout rate, number of units in fully connected layers, loss functions, optimizer, and various learning rates for 100 epochs each. We used the extended version of the Cornell dataset [21] comprising 1035 RGB-D images of 240 household objects. In this work, we considered the 5110 positive grasp configurations and discard all the negative labels. Furthermore, since the Cornell dataset is a small dataset, we augmented the data by zooming, random cropping, and rotating functions to generate 51100 images. The augmented dataset is then used to train the network. We report the obtained results based on the Intersection over Union (IoU) metric, and speed. A grasp pose is considered as a valid grasp if the intersection of the predicted grasp rectangle and the grand truth rectangle is more than 25%, and the orientation difference between predicted and grand truth grasp rectangles is less than 30 degrees. The final architecture is shaped as: $C_{(9 \times 9 \times 8, S_3)}$, $C_{(5 \times 5 \times 16, S_2)}$, $C_{(5 \times 5 \times 16, S_2)}$, $C_{(3 \times 3 \times 32)}$, $C_{(3 \times 3 \times 32)}$, $C_{(3 \times 3 \times 32)}$, $T_{(3 \times 3 \times 32)}$, $T_{(3 \times 3 \times 32)}$, $T_{(3 \times 3 \times 32)}$, $T_{(5 \times 5 \times 16, S_2)}$, $T_{(5 \times 5 \times 32, S_2)}$, $T_{(9 \times 9 \times 32, S_3)}$, where S stands for strides. We used Adam optimizer with a learning rate of 0.001, and Mean Squared Error as a loss function. The number of trainable parameters of our network is 116K, which makes it suitable for closed-loop control at the rate of up to 45 Hz.

We compared our approach with six visual grasp detection baselines, including Jiang et al. [22], Lenz et al. [5], Redmon et al. [23], Wang et al. [24], GG-CNN [6], and GG-CNN2 [2]. Results are reported in Table I. Our approach achieved state-of-the-art performance and outperformed the selected approaches by a large margin. Concerning IoU metric, our approach achieved 89.51% which was 28.81, 15.61, 4.21, 1.51, 16.51, and 14.31 percentage point (p.p) better than Jiang et al. [22], Lenz et al. [5], Redmon et al. [23], Wang et al. [24], GG-CNN [6], and GG-CNN2 [2] respectively. In addition to the IoU metric, we also computed the average grasp prediction time for each of the mentioned approaches. The obtained results indicated that Jiang et al. [22], Lenz et al. [5], Redmon et al. [23], and Wang et al. [24] methods need a very long time to predict grasp poses for a given object. Hence, these approaches are computationally expensive, and not useful for real-time robotic applications, where a closed-loop controller

TABLE I
RESULT OF OBJECT GRASPING ON THE CORNELL DATASET [22].

approach	input data	IoU (%)	speed (ms)
Jiang et al. [22]	RGB-D	60.7	5000
Lenz et al. [5]	RGB-D	73.9	1350
Wang et al. [24]	RGB-D	85.3	140
Redmon et al. [23]	RGB-D	88.0	76
GG-CNN [6]	depth image	73.0	19
GG-CNN2 [2]	depth image	75.2	21
Our approach	depth image	89.51	22

is usually needed. In contrast, the inference times for the GG-CNN [6], GG-CNN2 [2], and our approach was less than 25 ms, which represents that these approaches are suitable for real-time object grasping (i.e., a closed-loop control can work steadily in ≥ 45 Hz). The underlying reason for fast inference is that these approaches use a relatively small CNN, while other selected approaches are based on very deep neural networks with millions of parameters. Although GG-CNN [6] and GG-CNN2 [2] achieved slightly better execution time than our approach (i.e., 3 ms, and 1 ms faster respectively), the grasp success rate of our approach achieved significantly better performance on the IoU metric.

B. Grasp evaluation

Our experimental setups are shown in Fig. 4. In this work, we have developed a simulation environment in Gazebo similar to our real-robot setup to extensively evaluate our approach. It should be noted that we had very limited access to the lab given the COVID-19 crisis. The robot and the camera in the simulated environment were placed according to the real-robot setup to obtain consistent performance. Our setup comprises a Universal Robot (UR5e) with a two-fingered Robotiq 2F-140 gripper, a Kinect V1 camera mounted on a tripod, and a user interface to start and stop the experiments. The robot worked in a closed-looped eye-to-hand scenario. The whole pipeline has been developed over ROS (melodic) in C++.

To evaluate the performance of the proposed approach, we designed (i) *isolated*, (ii) *packed*, and (iii) *pile* removal tasks (see Fig. 5). In each round, we randomly generated a new scene consisting of four to six objects in the case of packed and pile scenarios, while for the isolated object scenario, we placed a randomly selected object in an arbitrary pose inside the robot’s work-space. In all experiments, the robot knows in advance about the pose of the *bin* object as the placing pose, while it has to detect and track the pose of target objects to be

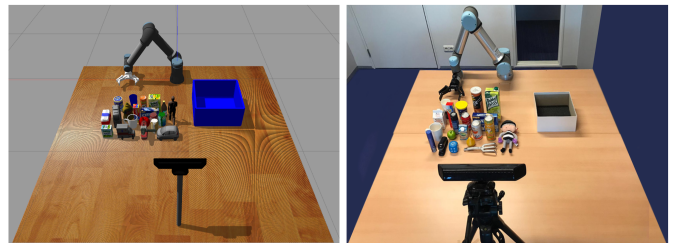


Fig. 4. Our experimental setups in: (left) simulation environment; and (right) the real-world setting. It should be noted, both simulated and real sets of objects used for evaluations are shown in these figures.



Fig. 5. Illustrative examples of three evaluation scenarios in Gazebo: (left) isolated object; (center) packed of objects; (right) pile of objects.

removed from the table. Afterward, the robot needs to predict grasp synthesis and select the best graspable pose of the target object, picks it up, and puts it in the *bin*. This procedure is repeated until all objects get removed from the table. Note that, at the beginning of each experiment, we set the robot to a pre-defined setting, and randomly place objects on the table. We used a set of 20 simulated objects, imported from different sources (e.g., the YCB dataset [25], Gazebo repository, and etc), and 20 real daily-life objects with different shapes, sizes, and weight (see Fig. 4). All objects were inspected to be sure that at least one side fits within the gripper. We assessed the performance of our approach by measuring success rate $= \frac{\text{number of successful grasps}}{\text{number of attempts}}$. We compared our approach with Grasp Pose Detection (GPD) [10] by performing the same experiments. Since GPD is a stochastic approach, it just requires a point cloud to generate grasps candidates.

1) *Isolated object scenario*: In this round of experiments, each object was tested in both real-world and simulation environments for 10 and 50 times, respectively. A particular grasp was recorded as a success if the object is inside the bin at the end of the experiment. The best grasp point is defined as the collision-free and kinematically feasible one with the highest grasp quality. Note that, to speed up the real-robot experiments, we randomly placed five objects on the table. In each execution cycle, the robot selected the nearest object to the base and tried to remove it from the table. Results are reported in Table II. By comparing both real and simulation experiments, it is visible that our approach outperformed GPD by a large margin. Particularly, in the case of simulation experiments, we achieved a grasp success rate of 89.7% (i.e., 897 success out of 1000 trials), while GPD obtained 78.7%. Figure 6 shows the best grasp configuration for 10 simulated objects. In the case of real-robot experiments, the success rate of our approach was 90.5% (181 success out of 200 attempts), which was 9.5% better than GPD (81%). The underlying reason was that the proposed approach generated grasp configurations per point, resulting in a diverse set of grasps for the target object, which we then selected the best kinematically feasible one. This is not the case for the GPD approach. More specifically, GPD generated a few grasps for a target object, and sometimes, none of the configurations led to a successful attempt. We observed that failed attempts were mainly due to inaccurate bounding box estimation, some objects in specific pose had a very low grasp quality score due to partially inaccurate depth

TABLE II
PERFORMANCE ON ISOLATED
SCENARIO

Method	Type	Success rate (%)
Our	sim	89.7 (897/1000)
GPD	sim	78.7 (787/1000)
Our	real	90.5 (181/200)
GPD	real	81.0 (162/200)

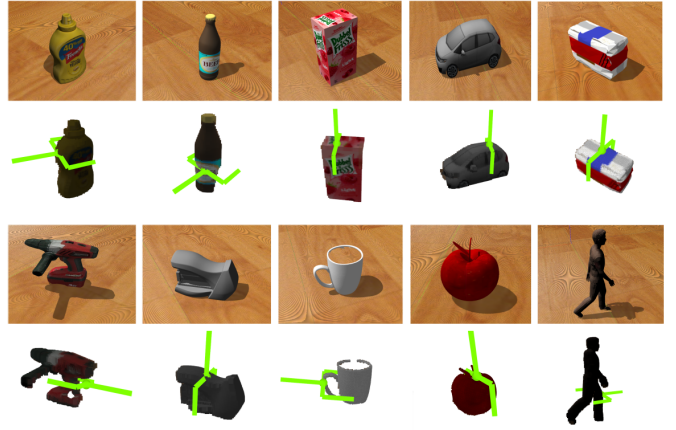


Fig. 6. Qualitative results for 10 never-seen-before household objects in the isolated scenario: visualizing objects in Gazebo and their best grasp configurations. These results showed that our approach learned very-well the intended object-agnostic grasp function.

map estimation, collisions between the gripper and the table mainly in top-down grasps, and collision between the object and the bin (mainly happened for large objects e.g., *Pringles* and *Juice box*). Another type of failure grasps occurred when one of the fingers of the gripper was tangent to the surface of the target object, which led to pushing the target object away instead of grasping.

2) *Pile and packed scenarios*: To generate a simulated scene containing a pile of objects, we randomly spawn objects into a box placed on top of the table. We wait for a couple of seconds until all objects become stable, and then remove the box, resulting in a cluttered pile of objects. To generate a packed scenario, we iteratively placed a set of objects next together in the workspace. An example for each scenario is shown in Fig. 5 (*center* and *right*). In the case of real-robot experiments, we randomly put four to six objects in a box, then shake the box to remove bias, and finally pour the box in front of the robot to make a pile of objects. In the case of packed experiments, we manually generate scenes by putting several objects together.

In this round of evaluation, in addition to the success rate, we report the average percentage of objects removed from the workspace.

TABLE III
PERFORMANCE ON PACKED SCENARIO

Method	Type	Success rate	Percent cleared
$\tau = 0.7$	sim	0.55 (142/260)	0.71 (142/200)
$\tau = 0.8$	sim	0.84 (176/210)	0.88 (175/200)
$\tau = 0.9$	sim	0.94 (141/150)	0.71 (141/200)
GPD	sim	0.54 (139/256)	0.70 (139/200)
$\tau = 0.8$	real	0.91 (38/42)	0.88 (38/40)
GPD	real	0.64 (31/48)	0.76 (31/40)

An experiment is continued until either all objects get removed from the workspace, or three failures occurred consecutively, or the quality of the grasp candidate is lower than a pre-defined threshold, τ . This parameter plays an important role. We performed 150 packed removal tests to tune the grasp quality threshold by setting $\tau \in \{0.7, 0.8, 0.9\}$, i.e., 50 simulation experiments for each τ . In each iteration, we randomly generated a scene including four objects. In each execution cycle, the robot is instructed to execute a collision-free and kinematically feasible grasp synthesis that has the maximum grasp quality. We also performed a set of

experiments with GPD. Results are reported in table III. It was observed that by setting $\tau = 0.9$, the robot could remove fewer objects from the workspace while achieving a higher success rate. In the case of $\tau = 0.7$, the success rate degraded by executing 118 unsuccessful grasp attempts. Experimental results showed that setting $\tau = 0.8$ leads to a good balance between success rate and percentage of object removal. Our approach outperformed the GPD with a large margin in both simulated and real robot experiments ($> 25\%$). On closer inspection of real-robot experiments, the proposed method could successfully grasp 38 objects out of 42 attempts, resulting in 91% success rate and 88% percent cleared, while GPD resulted in 64% and 76% success rate and percent cleared, respectively. We found that unsuccessful grasps mainly occurred due to a collision between the gripper and the target object because of a small error in the estimation of objects' pose. Furthermore, we observed that mug-like objects are difficult for GPD and the target object mostly slipped out of the gripper during the manipulation phase. Based on these results, we realized that the proposed approach is able to predict meaningful grasp quality scores for a given scene/object. Figure 7 illustrates four examples of packed removal experiments.

Similar to the packed removal experiments, we performed simulation and real-robot tests to examine the performance of

the proposed approach in the pile of objects scenario. Results are summarized in Table IV. We explain the obtained results using an example. Figure 8 depicts a successful sequence of removing a pile of four objects using the proposed approach. It was observed that after removing *Mustard* and *Colgate* objects from the workspace (Fig. 8 *a, b*), the complexity of the scene reduced significantly. Therefore, the robot could find more grasp configurations whose grasp quality exceeds the threshold (Fig. 8 *c, d*). As shown in this example, while the robot was interacting with an object, the pose of the other objects changed completely, resulting in a situation that the target object is not graspable (e.g., toppled *Oreo* box). Such a situation was one of the main reasons for unsuccessful attempts. Some other failures occurred due to the lack of friction, applying limited force to the object,

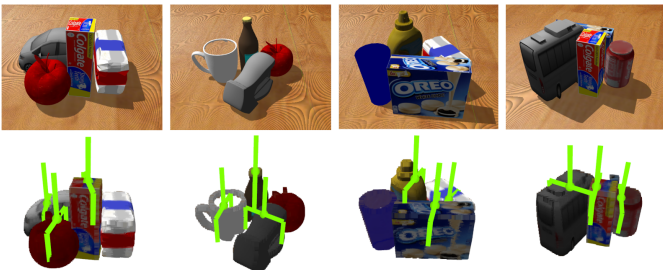


Fig. 7. Qualitative results on packed scenarios: visualizing the top-three grasp configurations on four different densely-packed objects.

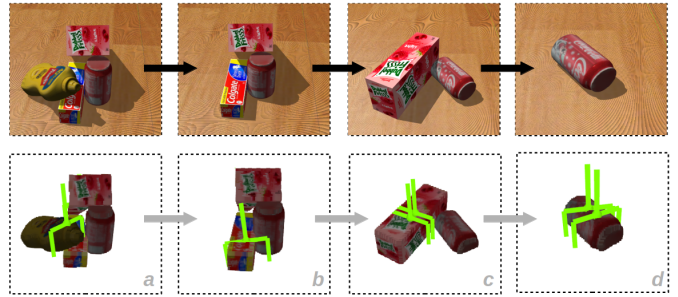


Fig. 8. An example of successful sequence of removing a pile of objects: in this experiment, the robot successfully removed *Mustard*, *Colgate*, *Juice box*, and *Coke can* objects one by one. In each execution cycle, grasp configurations that are collision-free and kinematically feasible are shown by green color.

collision with other objects, and unstable grasps predictions. In the case of computation time, our approach on average requires less than 25ms, while GPD needs more than 1.3s. A video summarizing these experiments is available online: <https://youtu.be/rBDEy5f7z0E>

V. CONCLUSION

In this paper, we proposed a deep learning approach for real-time multi-view 3D object grasping in highly cluttered (human-centric) environments. We trained the approach in an end-to-end manner. The proposed approach allows robots to robustly interact with the environments in both isolated and highly crowded scenarios. In particular, for a given scene, our approach first generates three orthographic views, The best view is then selected and fed to the network to predict a pixel-wise grasp configuration for the given object. The robot is finally commanded to execute the highest-ranked grasp synthesis. To validate the performance of the proposed method, we performed extensive sets of real and simulation experiments in three scenarios: *isolated*, *packed*, and *pile of objects*. Experimental results showed that the proposed method worked very well in all three scenarios, and outperformed the selected state-of-the-art approaches. In the continuation of this work, we would like to investigate the possibility of improving grasp performance by learning a shape completion function that receives a partial point cloud of a target scene and generates a complete model. We then use the full model of the object to estimate grasp synthesis map.

REFERENCES

- [1] J. Mahler, J. Liang, S. Niyaz, M. Laskey, R. Doan, X. Liu, J. A. Ojea, and K. Goldberg, "Dex-net 2.0: Deep learning to plan robust grasps with synthetic point clouds and analytic grasp metrics," *arXiv preprint arXiv:1703.09312*, 2017.
- [2] D. Morrison, P. Corke, and J. Leitner, "Learning robust, real-time, reactive robotic grasping," *The International Journal of Robotics Research*, vol. 39, no. 2-3, pp. 183–201, 2020.
- [3] J. Bohg, A. Morales, T. Asfour, and D. Kragic, "Data-driven grasp synthesis—a survey," *IEEE Transactions on Robotics*, vol. 30, no. 2, pp. 289–309, 2013.
- [4] D. Kalashnikov, A. Irpan, P. Pastor, J. Ibarz, A. Herzog, E. Jang, D. Quillen, E. Holly, M. Kalakrishnan, V. Vanhoucke *et al.*, "Qt-opt: Scalable deep reinforcement learning for vision-based robotic manipulation," in *Conference on Robot Learning*, 2018.
- [5] I. Lenz, H. Lee, and A. Saxena, "Deep learning for detecting robotic grasps," *The International Journal of Robotics Research*, vol. 34, no. 4-5, pp. 705–724, 2015.

- [6] D. Morrison, P. Corke, and J. Leitner, "Closing the Loop for Robotic Grasping: A Real-time, Generative Grasp Synthesis Approach," in *Proc. of Robotics: Science and Systems (RSS)*, 2018.
- [7] M. Breyer, J. J. Chung, L. Ott, S. Roland, and N. Juan, "Volumetric grasping network: Real-time 6 dof grasp detection in clutter," in *Conference on Robot Learning*, 2020.
- [8] Y. Li, L. Schomaker, and S. H. Kasaei, "Learning to grasp 3D objects using deep residual u-nets," in *2020 29th IEEE International Conference on Robot and Human Interactive Communication (RO-MAN)*. IEEE, 2020, pp. 781–787.
- [9] H. Liang, X. Ma, S. Li, M. Görner, S. Tang, B. Fang, F. Sun, and J. Zhang, "Pointnetgpd: Detecting grasp configurations from point sets," in *2019 International Conference on Robotics and Automation (ICRA)*. IEEE, 2019, pp. 3629–3635.
- [10] M. Gualtieri, A. Ten Pas, K. Saenko, and R. Platt, "High precision grasp pose detection in dense clutter," in *2016 IEEE/RSJ International Conference on Intelligent Robots and Systems (IROS)*. IEEE, 2016, pp. 598–605.
- [11] A. Kanezaki, Y. Matsushita, and Y. Nishida, "RotationNet: Joint object categorization and pose estimation using multiviews from unsupervised viewpoints," in *Proceedings of the IEEE Conference on Computer Vision and Pattern Recognition*, 2018, pp. 5010–5019.
- [12] C. R. Qi, H. Su, M. Nießner, A. Dai, M. Yan, and L. J. Guibas, "Volumetric and multi-view CNNs for object classification on 3D data," in *Proceedings of the IEEE conference on computer vision and pattern recognition*, 2016, pp. 5648–5656.
- [13] B. Shi, S. Bai, Z. Zhou, and X. Bai, "Deeppano: Deep panoramic representation for 3-d shape recognition," *IEEE Signal Processing Letters*, vol. 22, no. 12, pp. 2339–2343, 2015.
- [14] A. Zeng, K.-T. Yu, S. Song, D. Suo, E. Walker, A. Rodriguez, and J. Xiao, "Multi-view self-supervised deep learning for 6d pose estimation in the amazon picking challenge," in *2017 IEEE international conference on robotics and automation (ICRA)*. IEEE, 2017, pp. 1386–1383.
- [15] X. Yan, J. Hsu, M. Khansari, Y. Bai, A. Pathak, A. Gupta, J. Davidson, and H. Lee, "Learning 6-DoF grasping interaction via deep geometry-aware 3D representations," in *2018 IEEE International Conference on Robotics and Automation (ICRA)*. IEEE, 2018, pp. 3766–3773.
- [16] D. De Gregorio, F. Tombari, and L. Di Stefano, "Robotfusion: Grasping with a robotic manipulator via multi-view reconstruction," in *European Conference on Computer Vision*. Springer, 2016, pp. 634–647.
- [17] D. Morrison, P. Corke, and J. Leitner, "Multi-view picking: Next-best-view reaching for improved grasping in clutter," in *2019 International Conference on Robotics and Automation (ICRA)*. IEEE, 2019, pp. 8762–8768.
- [18] A. ten Pas, M. Gualtieri, K. Saenko, and R. Platt, "Grasp pose detection in point clouds," *The International Journal of Robotics Research*, vol. 36, no. 13-14, pp. 1455–1473, 2017.
- [19] S. H. Kasaei, L. Seabra Lopes, and A. Tomé, "Local-LDA: Open-ended learning of latent topics for 3D object recognition," *IEEE transactions on pattern analysis and machine intelligence*, 2019.
- [20] S. H. Kasaei, N. Shafii, L. Seabra Lopes, and A. M. Tomé, "Object learning and grasping capabilities for robotic home assistants," in *RoboCup 2016: Robot World Cup XX*. Springer International Publishing, 2017, pp. 279–293.
- [21] Y. Jiang, S. Moseson, and A. Saxena, "Efficient grasping from RGBD images: Learning using a new rectangle representation," in *IEEE International conference on robotics and automation*. IEEE, 2011, pp. 3304–3311.
- [22] —, "Efficient grasping from RGBD images: Learning using a new rectangle representation," in *2011 IEEE International conference on robotics and automation*. IEEE, 2011, pp. 3304–3311.
- [23] J. Redmon and A. Angelova, "Real-time grasp detection using convolutional neural networks," in *2015 IEEE International Conference on Robotics and Automation (ICRA)*. IEEE, 2015, pp. 1316–1322.
- [24] Z. Wang, Z. Li, B. Wang, and H. Liu, "Robot grasp detection using multimodal deep convolutional neural networks," *Advances in Mechanical Engineering*, vol. 8, no. 9, 2016.
- [25] B. Calli, A. Singh, J. Bruce, A. Walsman, K. Konolige, S. Srinivasa, P. Abbeel, and A. M. Dollar, "Yale-cmu-berkeley dataset for robotic manipulation research," *The International Journal of Robotics Research*, vol. 36, no. 3, pp. 261–268, 2017.